JCTC Journal of Chemical Theory and Computation

Article

pubs.acs.org/JCTC

How the Intercalation of Phenanthroline Affects the Structure, Energetics, and Bond Properties of DNA Base Pairs: Theoretical Study Applied to Adenine−Thymine and Guanine−Cytosine Tetramers

Adrià Gil,*[,†] Manuel Melle-Franco,[‡] Vicenç Branchadell,[§] and Maria José Calhorda*[,†]

[†]Centro de Química e Bioquímica, DQB, Faculdade de Ciências, Universidade de Lisboa, Campo Grande, 1749-016 Lisboa, Portugal

[‡]Centro ALGORITMI, Universidade do Minho, 4710-057 Braga, Portugal

[§]Departament de Química, Universitat Autònoma de Barcelona, 08193 Bellaterra, Barcelona, Spain

Supporting Information

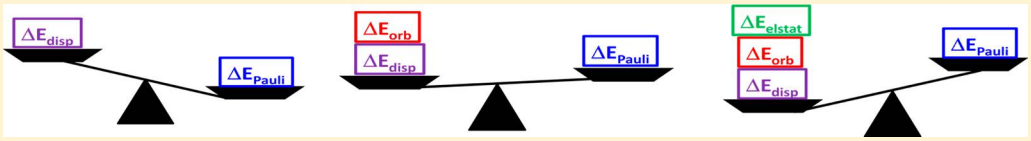

ABSTRACT: The effects of phenanthroline (phen) intercalation on the structure, energetics, and bonding of adenine−thymine and guanine−cytosine tetramers (A−T/T−A and G−C/C−G) were studied through density functional theory (DFT) using functionals that were recently improved to consider the effect of dispersion forces. Our results given by energy decomposition analysis show that the dispersion contribution, ΔE_{disp}, is the most important contribution to the interaction energy, ΔE_{int}. However, it is not enough to compensate the Pauli repulsion term, ΔE_{Pauli}, and the roles of the orbital contribution, ΔE_{orb}, and, in particular, the electrostatic contribution, ΔE_{elstat}, become crucial for the stabilization of the structures in the intercalation process. On the other hand, for G−C/C−G systems, hydrogen-bonding (HB) interactions are more important than stacking (S) interactions, whereas for A−T/T−A systems, HB and S become competitive. Moreover, intercalation produces important changes not only in the hydrogen bonds of base pairs, because S and HB are deeply connected, but also in other characteristic geometric parameters of the base pairs.

INTRODUCTION

Since the introduction of cisplatin in chemotherapy treatments for cancer,[1] interest in the application of inorganic (and organometallic) complexes in medicine has grown rapidly. One step beyond this was taken by the incorporation of 1,10-phenanthroline (phen) ligand (Scheme 1) in organometallic complexes, with these systems showing significant antitumoral activity.[2−6] In particular, its Mo(II) complexes were effective *in vitro* against different human tumor cell lines.[2] Among the interactions of organometallic complexes with DNA, intercalation is an important binding mode[7] and is influenced by the planarity of the ligand, type of donor atom, and metal coordination geometry.[8] Several reviews addressing the intercalation of one ligand of a metal complex between base pairs of DNA have appeared recently.[9−13]

Recent experimental studies on the interaction of organometallic systems containing phen with DNA, which are based on techniques such as circular dichroism, fluorescence, quenching processes, and thermal denaturation, are consistent with the partial intercalation of this planar ligand between DNA base pairs.[3,14] Viscosity, linear dichroism, and NMR and NOESY spectra experiments also showed that methylated derivatives of phen and dipyrido[3,2-a:2′,3′-c]phenazine (dppz) ligand (Scheme 1) also intercalate between DNA base pairs.[15,16] Moreover, very recently determined crystal structures showed how the dppz ligand of $[Ru(tap)_2(dppz)]^{2+}$, $[Ru(bpy)_2(dppz)]^{2+}$, and $[Ru(phen)_2(dppz)]^{2+}$ complexes interacts with DNA duplex chains.[17−20]

Many studies have also been carried out over the last 15 years to model the interaction of molecules in DNA from a theoretical point of view,[21−41] using several approaches. On one hand, large systems were treated by the use of force fields in molecular mechanics (MM) or classical molecular dynamics (MD). Trieb et al.[21] studied the intercalation of daunomycin

Scheme 1

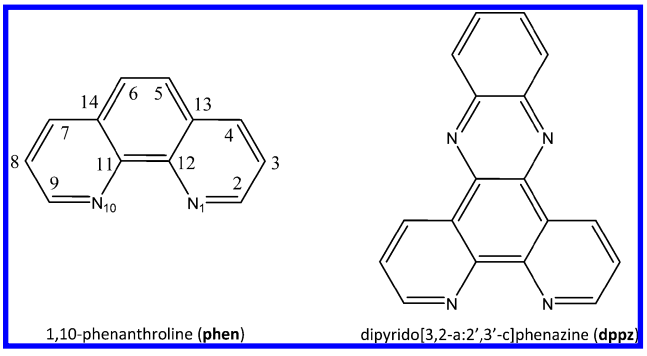

Received: July 14, 2014
Published: May 12, 2015

DOI: 10.1021/ct5006104
J. Chem. Theory Comput. 2015, 11, 2714−2728

between DNA base pairs by MD, a continuum solvent method, and the use of the DNA sequence d(CGCGCGATCG-CGCG)$_2$, whereas Mukherjee et al.[22] used the d(GCGC-ACGTGCGC)$_2$ DNA sequence to study the intercalation of daunomycin by MD and umbrella sampling techniques. One step beyond this was given in the study of Robertazzi et al.,[23] in which not only the intercalator (phen) but also the whole organometallic complex was taken into account in the simulation by using several Cu complexes and the B-DNA fragment d(GGCCCTTATCAGGGC)$_2$ to describe the Cu(I) complexes mode of binding to DNA by steered MD simulations. Vargiu et al.[24] analyzed the intercalation and insertion of several Rh complexes containing chrysi, dppz, and eilatin ligands into the DNA dodecamer d(CGGAAATTC-CCG)$_2$ via force field based MD, and they improved the approach with some quantum classical (QM/MM) MD simulations. Also, Galindo-Murillo et al.[25] carried out MD to find the preferred site of binding between [Cu(2,2′-bipyridine)-(acetylacetonate)(H_2O)]$^+$ and four selected DNA chains: (AAAAAAAAAA)$_2$, (ATATATATAT)$_2$, (GGGGGGGGGG)$_2$, and (GCGCGCGCGC)$_2$. Moreover, more recently, Sasikala et al.[26] used well-tempered metadynamics with multiple collective variables to calculate the free energy landscapes of intercalation, deintercalation, and dissociation processes through both the major and minor grooves using proflavine intercalator with the d(GCGCTCGAGCGC)$_2$ sequence of DNA solvated with water by the TIP3P model. Also, very recently, Franco et al.[27] analyzed the deintercalation mechanism of Δ-[Ru-(bpy)$_2$(dppz)]$^{2+}$ and Δ-[Rh(bpy)$_2$(chrysi)]$^{3+}$ complexes by MD simulations with the 5′-d[CGGAAATTCCCG]-3′ DNA sequence solvated with explicit water molecules by the TIP3P model. On the other hand, small systems have been treated at a high level of theory. Early examples include the study of Bondarev et al.,[28] in which the nature of the stacking interactions for the intercalator amiloride and the Watson−Crick base pairs (AT and GC) was studied using a model with one base pair and the intercalator at the MP2/6-31++G(d,p) level. Another seminal example is that of Řeha et al.,[29] who investigated the stacking interactions of the intercalators ethidium, daunomycin, elipticine, and 4,6′-diaminide-2-phenyl-indole with AT and GC base pairs at several levels of theory, MP2/6-31G*(0.25) and DFTB-D, which yielded the most accurate results. Also, Kumar et al.[30] used the DFTB-D method and compared the results for stacking energies to MP2/6-31G* results in their study regarding the interaction of benzo[*a*]-pyrene and its metabolites with the GC base pair by means of a three-body model with the base pair and the intercalator. This three-body model was also used in the recent work of El-Gogary et al.,[31,32] who addressed the interaction of psoralen and 8-methoxypsoralen with DNA Watson−Crick base pairs (AT and GC) using several methods: HF, B3LYP, and MP2 with different basis sets. Also, in a recent study carried out by Hazarika et al.,[33] this model with one base pair and the intercalator was used. In this case, different levels of theory allowed the favorable regions for the stacking interaction of phen with base pairs AT and GC to be predicted, and the results of MP2/6-31+G(d,p) were found to be reasonable for monitoring such interactions. Finally, Li et al.[34] studied the relationship between stacking interactions and the intercalation of proflavine and ellipticine within DNA using a nonempirical van der Waals density functional for the correlation energy in a model consisting of the base pair (AT or GC) and the intercalator. There are other approximations in the literature between the treatment of a DNA sequence of various steps and the intercalator at a low level of theory and the treatment of the three-body system with the base pair and the intercalator at a high level of theory. Xiao et al.,[35] based on a model consisting of the intercalator and two base pairs, replaced the desoxyribose rings by methyl groups and used HF/6-31G* and MP2/6-31G levels of theory to predict the orientation of indenoisoquinoline in the ternary cleavage complex formed from DNA and topoisomerase I (top1). Langner et al.[36] analyzed the interaction energies between ethidium and proflavine intercalators and their four nearest bases at the MP2/6-31G(d,p) level of theory. Hill et al.[37] took into account a similar approach to analyze the interaction energies for the binding of ellipticine, ethidium, and daunomycin intercalators to base-pair steps (GC/CG and AT/TA). On the other hand, the structural and spectroscopic properties of [Ru(phen)$_2$(dppz)]$^{2+}$ and [Ru-(tap)$_2$(dppz)]$^{2+}$ were investigated with another approximation (DFT and TD-DFT methods within the polarized continuum model and QM/MM calculations in which the QM part included the Ru complexes, whereas the basis pairs, sugars, and phosphates were taken into account in the MM part) by Ambrosek et al.[38] Also, Biancardi et al.[39] studied some spectroscopic properties of cyanine thiazole orange (TO) intercalated in DNA using two models: the smallest model (Sandwich), in which TO and the four adjacent nucleic acid bases were considered, and the larger model (Ring), in which sugar/phosphate groups were also taken into account. The ground- and excited-state geometry optimizations were calculated with DFT and TD-DFT methods with the M06-2X functional to include dispersion contributions. Hohenstein et al.[40] carried out DF-SAPT0 calculations on the intercalation of DNA by proflavine on a model consisting not only of a CG step with the intercalator but also with an AT base pair added near the intercalation site. Finally, the very recent work of Deepa et al.[41] should be cited, in which the authors tried to understand the physicochemical interaction between psoralen and altretamine with stacked DNA base pairs using a model that consisted of the intercalator and the four DNA bases along with the sugar phosphate backbone at the M05-2X/6-31G* level of theory, among others.

These examples show how the growing interest in using these systems for a range of medical applications has prompted a renewed need for a structural understanding of their interactions with the bases of DNA.[42] 1,10-Phenanthroline plays a central role here, as it is, along with many of its derivatives, an intercalator, so it is desirable to develop a strategy to understand this process and calculate the energy terms by accounting for its interaction with DNA base pairs. This aim can be achieved by the use of quantum chemistry calculations, and, in this work, we address the study of phen intercalation between the A−T/T−A and G−C/C−G stacked base pairs of DNA by means of DFT calculations with recently developed functionals that take into account dispersion forces, which are crucial for the study of intercalation. In order to do this, we used a model consisting of the intercalator (phen) and two DNA base pairs (A−T/T−A and G−C/C−G), and we based our study on the results of the M06-2X functional,[43,44] which takes dispersion forces into account. Besides discussing the geometries and energy partitioning, interactions and bond properties are analyzed in terms of dipolar moment, polarizability, electronic density, charge transfer, molecular electrostatic potential (MEP) maps, and frontier orbitals. As far as we know, this is the first study to address the role of the different

DOI: 10.1021/ct5006104
J. Chem. Theory Comput. 2015, 11, 2714−2728

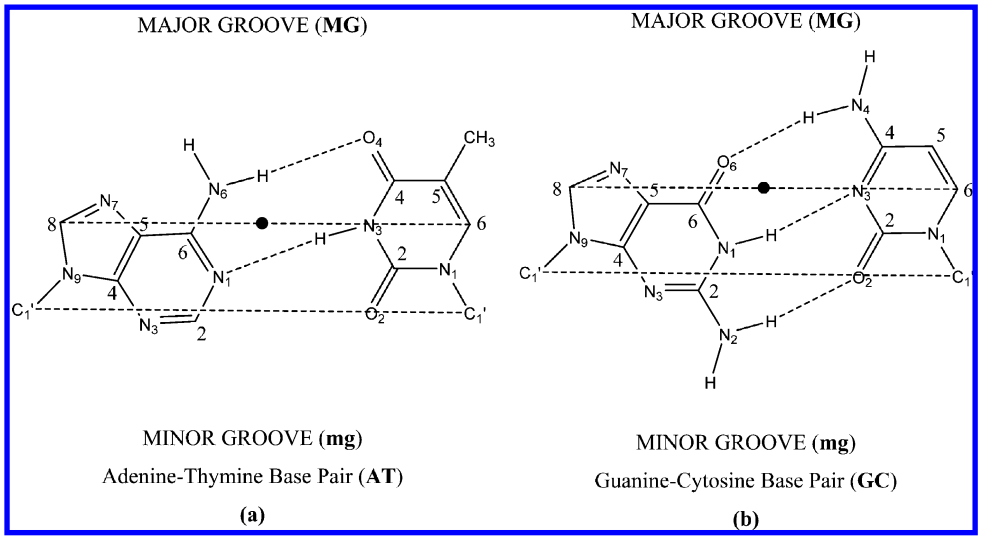

Figure 1. Scheme of the A−T (a) and G−C (b) base pairs. The dashed line C_6-C_8 represents the long base pair axis, which is roughly parallel to the $C_1'-C_1'$ line (C_1' stands for the sugar carbon atoms bonded to the bases). The twist angle (θ) is defined as the rotation around the midpoint of the C_6-C_8 axis (denoted by a dot).

energy contributions to the interaction energy in a system of four DNA bases and an intercalator using DFT methods that take into account the role of dispersion forces. Moreover, although gas-phase calculations may seem to be too far from physiological systems, knowledge of intrinsic molecular interactions can be very useful and constitutes an important prerequisite toward understanding the role of intercalators between nucleobases in the DNA structure. Moreover, they are also used to develop force fields. Thus, we expect that this study will help to understand how phen ligand, which is a precursor to other intercalators, evolves in biological processes of intercalation and the role that the interactions involved in such processes have; in addition, this understanding will help to interpret the results of several experimental techniques.

COMPUTATIONAL METHODS

The standard method for introducing dispersion energy is the combination of MP2 theory in the complete basis set (CBS) limit with a ΔCCSD(T) correction computed in a smaller basis to estimate the CBS CCSD(T) results.[45−48] However, this approach is prohibitive when studying large systems of biological interest. As an alternative, methods based on DFT that include dispersion correction can be used. Some functionals proposed by Truhlar and co-workers[43] include this correction implicitly. In particular, M06-2X[43,44] is very adequate for the study of noncovalent interactions, and several authors have emphasized the good performance of the M06-2X method,[49−53] although some others have shown that it has some limitations.[54,55]

Thus, M06-2X was chosen for our calculations, and, following the recommendation of Truhlar et al.,[56] the 6-31+G(d,p) basis set[57] was used. Calculations were performed with the Gaussian 09 package.[58] Optimizations were carried out without any constraint on a model based on the two stacked base pairs and the phen molecule between the two pairs (sandwich model).[39] We started with the optimized geometries of A−T/T−A (θ = 36°) and G−C/G−C from refs 59 and 60, respectively, which correspond to Watson−Crick base pairing found in DNA. We increased the distance between the two base pairs, defined as the rise parameter, *R*, of Olson et al.[61] (*z* coordinate), to twice the initial value, and we inserted manually the intercalator between both base pairs in such a way that the distance from phen to any of the two base pairs was the same (about 3.4 Å) and that the overlap between base pairs and phen was maximized. Two different orientations were taken into account for the model system (intercalator + four DNA bases): the orientation in which the intercalation takes place from the major groove (this situation is reproduced in our model when the N atoms of phen ligand are close to the major groove; see Figure 1 to locate the side corresponding to the major groove in the base pairs) and the orientation in which the intercalation of the system is produced from the minor groove (situation reproduced when N atoms of phen are close to the minor groove; see Figure 1 to locate the side corresponding to the minor groove in the base pairs). The structures corresponding to these two orientations will be called (A−T/phen/T−A)MG (intercalation from major groove) and (A−T/phen/T−A)mg (intercalation from minor groove) for the systems containing adenine and thymine and (G−C/phen/C−G)MG (intercalation from major groove) and (G−C/phen/C−G)mg (intercalation from minor groove) for the systems with guanine and cytosine (Figure 2 shows these four systems after optimization).

All optimized geometries have been characterized by calculating the harmonic vibrational frequencies to verify that all frequencies are real and that the structures correspond to minima in the potential energy surface. For some calculations, we used the counterpoise method[62,63] to estimate the basis set superposition error (BSSE). Following Šponer et al.'s recommendation,[64] charges were derived from the natural bond orbital method (NBO)[65,66] by means of NBO 5.0. software[67] to quantify the charge transfer during the intercalation process. The identification of bond critical points[68] and the topological analysis were carried out using the AIM2000 program.[69]

Energy decomposition analysis (EDA), as implemented in the ADF program,[70−72] was used to calculate the contribution of the different energy terms to the interaction energy between the fragments. In this analysis, the interaction energy ΔE_{int} is split into contributions associated with orbital (ΔE_{orb}), Pauli (ΔE_{Pauli}), and electrostatic (ΔE_{elstat}) terms following a

DOI: 10.1021/ct5006104
J. Chem. Theory Comput. 2015, 11, 2714−2728

Morokuma-type energy decomposition method.[73,74] These calculations were also carried out with the M06-2X functional and an uncontracted polarized triple-ζ basis set of Slater-type orbitals (TZP). Due to convergence problems with M06-2X, we also carried out the EDA with the M06-L[75] functional and the B3LYP-D3 functional with the explicit Grimme's D3 correction to dispersion forces,[76−79] both of which are also included in the ADF software, and the TZP basis set. Moreover, to have some guide regarding the accuracy of the calculation of the interaction energy, we also carried out MP2 single-point calculations (Gaussian09) with a 6-31*(0.25) basis set. In this basis set, the energy-optimized d-polarization functions were changed to dispersion energy optimized ones with a more diffuse exponent of 0.25 for C, N, and O atoms (the standard exponent is 0.8).[29,80] As stated in the literature,[81] results from MP2 calculations using the 6-31G*(0.25) basis set have been found to be closer to the CCSD(T) values. In light of these observations, MP2/6-31G*(0.25) calculations can provide us with a high-quality benchmark value for systems where no reference is available.

For some systems, (G−C/phen/C−G)MG and (G−C/phen/C−G)mg, we also included the DNA backbone with the sugars and phosphates belonging to the intercalation pocket to determine its influence on geometries and on the energetic terms of EDA. Moreover, Na^+ cations were also taken into account to balance the negative charge of the phosphates. Because of the increased size of the system when sugars, phosphates, and Na^+ cations are added, we optimized with the PM6-DH2 method,[82] which includes corrections for dispersion forces, using MOPAC2012 software.[83,84] PM6-DH2 has been found to give a reasonable representation of stacking interactions[85] and gave comparable geometries to those with DFT-D methods in the studied (A−T/phen/T−A)MG, (A−T/phen/T−A)mg, (G−C/phen/C−G)MG, and (G−C/phen/C−G)mg systems without sugars and phosphates.[86]

RESULTS AND DISCUSSION

As mentioned previously, we carried out complete DFT optimizations of several structures of A−T/T−A and G−C/C−G base pairs incorporating phen and using the M06-2X functional, and in the following sections, we shall discuss some geometry parameters of the optimized structures and energetics as well as other properties related to bonding properties such as dipole moment, polarizabilities, electronic densities, charge transfer, MEPs, and frontier orbitals.

Geometric Parameters. The Cartesian coordinates of all of the optimized structures are available as Supporting Information. The structures of all systems optimized at the M06-2X/6-31+G(d,p) level of calculation are shown in Figure 2, from both a lateral view and above.

The lateral view more clearly shows the rise (R) displacement in the base pairs, whereas the view from above is better to appreciate the twist (θ) movement.[61] Aside from these two geometric parameters, we also focused on the analysis of the hydrogen-bond lengths between base pairs. In order to study the mean distance between the two base pairs, we defined the xy plane by the two atoms forming the $N_1\cdots N_3$ hydrogen bond and, as a third atom, the C_2 of adenine (adenine and thymine pairs) or the C_2 atom of cytosine (guanine and cytosine pairs), as shown in Figure 1. The R mean distance is then the difference between the mean z value of the atoms of the upper base pair and the one of the atoms of the lower base pair. Similarly, we calculated the mean distance between phen and

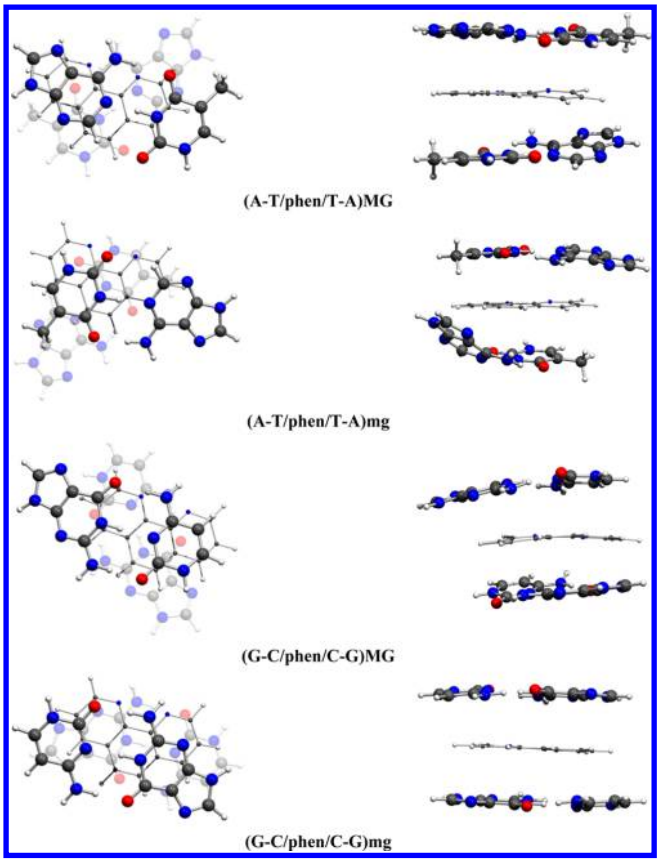

Figure 2. Optimized structures of the (A−T/phen/T−A)MG, (A−T/phen/T−A)mg, (G−C/phen/C−G)MG, and (G−C/phen/C−G)mg systems at the M06-2X/6-31+G(d,p) level of calculation, from both a lateral view (right) and above (left).

the base pairs. The θ coordinate of Olson et al.[61] can be defined from the schemes shown in Figure 1. The dashed line joining the C_8 atom of the purine base to the C_6 atom of the pyrimidine is the long base pair axis, and the θ coordinate is the rotation of one base pair around the center of its C_6-C_8 axis. Since the base pairs are not strictly planar and parallel after optimization, in order to quantify the rotation of the bases, the θ coordinate of the optimized structures is defined as the θ angle between the projections on the xy plane of the C_6-C_8 axis of each base pair. Thus, our θ twist angle would be the dihedral angle between the vector in the C_6-C_8 direction of the i base pair and the vector in the C_6-C_8 direction of the $i+1$ base pair in any step of the DNA chain.

The values of θ, R, the distance between phen and the base pairs, and the hydrogen-bond lengths for the upper and lower pairs of bases are presented in Table 1 for the four structures incorporating phen. Parameters for the stacked systems without phen are also included for comparison.

Let us analyze first the θ coordinate for the systems with adenine, thymine, and phen (Figure 2 and Table 1). Important changes are noticed for this θ parameter when intercalation occurs, and the θ angle increases by 19.4° and 17.1° for intercalation from the minor and major grooves, respectively. For the systems with guanine and cytosine, an important increase of 21.2° is observed for the θ angle in the (G−C/phen/C−G)MG system, whereas no appreciable variation is observed for the (G−C/phen/C−G)mg system. Thus, intercalation of phen produces an increase of the θ parameter

DOI: 10.1021/ct5006104
J. Chem. Theory Comput. 2015, 11, 2714−2728

Table 1. Hydrogen bond Lengths, Rise (R), Distance Phen···Base Pair, and Twist (θ) Optimized Parameters at the M06-2X/6-31+G(d,p) Level of Calculation[a]

structures	purine···pyrimidine	distance	d(X···H)[b]	R	d(phen···base pair)	θ
A−T/T−A	N_6···O_4	2.93/2.99	1.91/1.97	2.98		48.8
	N_1···N_3	2.81/2.78	1.76/1.73			
	C_2···O_2	3.53/3.38	2.77/2.57			
(A−T/phen/T−A)MG	N_6···O_4	2.98/3.00	1.98/1.99	5.99	3.12/2.87	65.9
	N_1···N_3	2.78/2.78	1.73/1.73			
	C_2···O_2	3.51/3.50	2.69/2.72			
(A−T/phen/T−A)mg	N_6···O_4	2.94/2.92	1.92/1.92	6.25[c]	3.10/3.14[c]	68.2
	N_1···N_3	2.78/2.84	1.73/1.82			
	C_2···O_2	3.47/3.49	2.65/2.72			
G−C/C−G	O_6···N_4	2.87/2.86	1.85/1.84	3.05		18.7
	N_1···N_3	2.93/2.93	1.90/1.90			
	N_2···O_2	2.88/2.88	1.86/1.86			
(G−C/phen/C−G)MG	O_6···N_4	2.85/2.86	1.82/1.83	5.85	3.00/2.84	39.9
	N_1···N_3	2.90/2.91	1.86/1.87			
	N_2···O_2	2.88/2.88	1.86/1.86			
(G−C/phen/C−G)mg	O_6···N_4	2.79/2.79	1.76/1.75	6.08	3.07/3.01	18.0
	N_1···N_3	2.92/2.92	1.89/1.89			
	N_2···O_2	2.94/2.94	1.93/1.93			

[a]Distances in angstroms, and angles in degrees. [b]X is N_1 of adenine, O_4 and O_2 of thymine, O_6 of guanine, and N_3 and O_2 of cytosine. [c]Only thymine was considered for the lower base pair because adenine is not stacked (Figure 2).

as a general trend with the exception of the (G−C/phen/C−G)mg system, for which no appreciable variation is observed.

Moving now to the R parameter, it varies from 2.98 Å for A−T/T−A systems (without phen) to 5.99 and 6.25 Å for (A−T/phen/T−A)MG and (A−T/phen/T−A)mg systems, respectively, which are roughly twice 2.98 Å. Interestingly, phen is not strictly equidistant from each base pair in the optimized structures, with the distances between phen and the upper and lower base pairs being 3.12 and 2.87 Å, respectively, in (A−T/phen/T−A)MG systems. In the case of (A−T/phen/T−A)mg systems, although the values given for the mean distance between phen and the base pairs are very similar in Table 1 (3.10/3.14 Å), one of the base pairs can be considered dislocated (one adenine is extruded), and the mean distance, in this case, was calculated only with respect to thymine. This preference of phen for thymine was already observed by Hazarika et al. in their recent study.[33] Also, it must be said that, in relation to the extrusion of the adenine base, this easy disruption of A−T base pairs was already mentioned in previous gas-phase studies.[87−89] On the other hand, for systems with guanine and cytosine, a similar trend is observed, and the system without phen has an R parameter of 3.05 Å, whereas the (G−C/phen/C−G)MG system has an R value of 5.85 Å and the (G−C/phen/C−G)mg system has a value of 6.08, which are both roughly twice 3.05 Å. It must be said that, for these systems with guanine and cytosine, phen can be considered equidistant in (G−C/phen/C−G)mg (3.07/3.01 Å) but not in (G−C/phen/C−G)MG (3.00/2.84 Å).

Interesting trends are also observed by looking at the lengths of the hydrogen bonds (Table 1). For systems with adenine and thyimine, the shortest hydrogen bond is N···H−N and the longest one is, as expected, the C−H···O hydrogen bond. This ordering correlates with the linearity of the hydrogen bonds, being 177.9°/173.6° for the upper/lower N···H−N, 173.0°/173.5° for the N−H···O, and 126.6°/131.0° for the C−H···O hydrogen bonds. When intercalation takes place from the major groove, the N−H···O distance increases for (A−T/phen/T−A)MG systems, whereas the N···H−N distance remains similar to the system without phen. On the other hand, the most important variation in the (A−T/phen/T−A)mg system is the lengthening of the N···H−N hydrogen bond, corresponding to the dislocated base pair, by about 0.1 Å. Nevertheless, despite the changes in hydrogen bonds, the initial ordering for strength of the systems without phen is maintained for the systems including it, with N···H−N being shorter than N−H···O and the latter being shorter than the C−H···O hydrogen bond. Again, the strength of the interaction, as measured by the distance, is related to the linearity of the hydrogen bond. In the case of the systems with guanine and cytosine, the shortest hydrogen bond corresponds to O···H−N and the longest to the N−H···N hydrogen bond. When intercalation takes place from the major groove, a shortening of O···H−N and N−H···N hydrogen bonds is observed for the (G−C/phen/C−G)MG system, whereas for the (G−C/phen/C−G)mg system, different behavior is observed for each hydrogen bond. The N−H···O bond lengthens by about 0.1 Å, N−H···N remains similar, and the O···H−N hydrogen bond shortens by about 0.1 Å. Thus, when intercalation takes place from the minor groove, the effect of intercalation is more important for the two lateral hydrogen bonds. It must also be mentioned that for G−C/C−G systems without phen the shortest hydrogen bond corresponds to O···H−N, whereas the longest is the N−H···N hydrogen bond. This ordering is maintained in (G−C/phen/C−G)MG systems but is different in (G−C/phen/C−G)mg systems, for which the shortest hydrogen bond corresponds to O···H−N but the longest corresponds to N−H···O. These results clearly show the important influence of intercalation on hydrogen bonds.

The effect of introducing the DNA backbone (sugars, phosphates, and Na^+ cations) was analyzed for the (G−C/phen/C−G)MG and (G−C/phen/C−G)mg systems. Such systems including the DNA backbone will be called bb(G−C/phen/C−G)MG and bb(G−C/phen/C−G)mg, and their optimized geometries at the PM6-DH2 level are shown in Figure 3, whereas the analyzed geometric parameters are depicted in Table 2.

DOI: 10.1021/ct5006104
J. Chem. Theory Comput. 2015, 11, 2714−2728

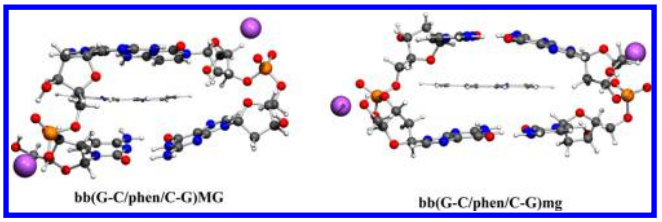

Figure 3. Optimized structures of the bb(G−C/phen/C−G)MG (left) and bb(G−C/phen/C−G)mg (right) systems at the PM6-DH2 level of calculation.

Looking at the studied geometrical parameters when the DNA backbone is included, no significant changes are observed when comparing the (G−C/phen/C−G)MG and (G−C/phen/C−G)mg systems to the bb(G−C/phen/C−G)MG and bb(G−C/phen/C−G)mg systems, respectively. Indeed, for the (G−C/phen/C−G)MG and bb(G−C/phen/C−G)MG systems, all hydrogen-bond distances are roughly similar, whereas for the (G−C/phen/C−G)mg and the bb(G−C/phen/C−G)mg system, the following order is obtained: O···H−N < N−H···N ∼ N−H···O. The value of the R parameter is higher for (G−C/phen/C−G)mg than for the (G−C/phen/C−G)MG system, and this trend is the same for the bb(G−C/phen/C−G)mg and bb(G−C/phen/C−G)MG systems. Finally, the θ parameter is very similar for the (G−C/phen/C−G)MG (39.9°) and bb(G−C/phen/C−G)MG (39.0°) systems and also for (G−C/phen/C−G)mg (18.0°) and bb(G−C/phen/C−G)mg (24.1°) systems.

Energies. The energy values for the studied structures are presented in Table 3. In this table, the first column (E_{tot}) corresponds to the total energy of the systems in atomic units, whereas the second column presents the energy of formation, E_f, defined as the energy difference between each system and twice the optimized base pairs A−T or G−C (systems without phen) or between each system and the sum of the optimized stacked pairs of bases (A−T/T−A or G−C/C−G) and isolated phen (systems with phen). The next column contains the interaction energy among bodies, $E_{int(bodies)}$, calculated by subtracting from the total energy the energy of all isolated units (four in A−T/T−A or G−C/C−G and five for the systems with phen) with the same geometry that they have in the complex. The energies in the three remaining columns were calculated with the geometries in the total system and analyzed by dividing the system into fragments in order to consider two-body and many-body interactions. E_{HB} is the two-body hydrogen-bonding interaction in each base pair, calculated as the difference between the energy of the base pair (A−T or G−C) and the sum of the energies of the two bases (A + T or G + C). E_S is the sum of the other four two-body interactions between the four bases. In the case of the systems without phen, we find two intrastrand and attractive stacking interactions and two interstrand and repulsive stacking interactions. Because the intrastrand interactions are higher than the interstrand interactions, the final balance gives a reduced attractive interaction for E_S. On the other hand, in the case of the systems with phen, the four two-body interactions between the four bases and phen included in E_S are always attractive. Finally, E_{MB} is the multibody interaction energy that was calculated by subtracting the two-body terms (E_{HB} and E_S) from the total interaction energy, $E_{int(bodies)}$.

We observe in Table 3 that $E_{int(bodies)}$ are, in all cases, more negative than E_f, as expected, given that the deformation energy is missing in $E_{int(bodies)}$. In the systems with phen, E_f are very similar in all cases (from −12 to −14 kcal mol^{-1}) with the exception of the (G−C/phen/C−G)mg system, for which E_f is −6.8 kcal mol^{-1}. The difference between $E_{int(bodies)}$ of the (G−C/phen/C−G)mg structure and (G−C/phen/C−G)MG is 7.7 kcal mol^{-1}. Thus, although the (G−C/phen/C−G)MG system is more distorted than (G−C/phen/C−G)mg (see geometrical parameters in Table 1 and see also Figure 2), the intercalation from major groove in (G−C/phen/C−G)MG leads to a higher $E_{int(bodies)}$ and thus E_f is more favorable for the (G−C/phen/C−G)MG system. The intercalation from the major groove leads to larger stabilizing interactions despite the deformation and distortion. $E_{int(bodies)}$ is always higher in the systems with guanine, cytosine, and phen than in the systems with adenine, thymine, and phen because the systems with guanine and cytosine have one more hydrogen bond than the systems with adenine and thymine and this additional interaction increases the value of $E_{int(bodies)}$. On the other hand, $E_{int(bodies)}$ is always higher when intercalation takes place from the major groove compared to that from the minor groove, although this difference is not appreciable for systems with adenine and thymine. Finally, it is worth mentioning that $E_{int(bodies)}$ is lower for systems without phen than it is for systems with phen. This is because the E_S contribution is more important in the systems with phen, as we shall see in the next paragraph. We also calculated the influence of the counterpoise (CP) correction in the values of $E_{int(bodies)}$ for all of the systems (Table 3). It amounts to 4.6 to 7.8 kcal mol^{-1} for systems with A−T, which represents between the 8.4 and 11.5% of $E_{int(bodies)}$, and from 6.8 to 8.8 kcal mol^{-1} for systems with G−C, which corresponds to 7.6 and 8.9% of $E_{int(bodies)}$. Thus, BSSE affects more systems with adenine and thymine, although, in general, BSSE does not change $E_{int(bodies)}$ dramatically at our level of calculation.

The analysis of the partition of $E_{int(bodies)}$ into two-body and many-body terms gives another perspective (see values in Table 3 and trends in Figure 4). For all of the systems, there are two similar values of E_{HB}, which correspond to the hydrogen bonds of the upper and lower pairs of bases. Nevertheless, we found

Table 2. Hydrogen Bond Lengths, Rise (R), Distance Phen···Base Pair, and Twist (θ) Optimized Parameters at the PM6-DH2 Level of Calculation[a]

structures	purine···pyrimidine	distance	d(X···H)[b]	R	d(phen···base pair)	θ
bb(G−C/phen/C−G)MG	O_6···N_4	2.85/2.90	1.81/1.86	6.02	2.97/3.05	39.0
	N_1···N_3	2.89/2.89	1.82/1.84			
	N_2···O_2	2.88/2.84	1.85/1.81			
bb(G−C/phen/C−G)mg	O_6···N_4	2.83/2.84	1.78/1.80	6.32	3.13/3.23	24.1
	N_1···N_3	2.91/2.89	1.85/1.83			
	N_2···O_2	2.94/2.88	1.93/1.84			

[a]Distances in angstroms, and angles in degrees. [b]X is O_6 of guanine and N_3 and O_2 of cytosine.

DOI: 10.1021/ct5006104
J. Chem. Theory Comput. 2015, 11, 2714−2728

Table 3. Total Electronic Energy at the M06-2X/6-31+G(d,p) Level of Calculation (Hartrees), Formation Energy, and Interaction Energies (kcal mol^{-1}) for the Free Stacked Base Pairs and Those Including Phen

structures	E_{tot}	E_f	$E_{int(bodies)}$ [a]	E_{HB}	E_S	E_{MB}
A−T/T−A	−1842.352161	−19.7	−54.4	−16.0/−16.4[b]	−22.6	0.5
			−49.9	(−32.4)		
(A−T/phen/T−A)MG	−2413.764878	−12.7	−67.8	−16.1/−15.8[b]	−34.0	−1.9
			−60.0	(−31.9)		
(A−T/phen/T−A)mg	−2413.763525	−11.9	−65.9	−16.4/−15.3[b]	−32.3	−2.0
			−58.6	(−31.7)		
G−C/C−G	−1874.461859	−23.8	−89.0	−31.3/−31.3[b]	−26.2	−0.2
			−82.2	(−62.6)		
(G−C/phen/C−G)MG	−2445.875685	−13.4	−103.0	−30.9/−31.0[b]	−38.7	−2.5
			−94.3	(−61.9)		
(G−C/phen/C−G)mg	−2445.865146	−6.8	−95.3	−31.1/−31.1[b]	−34.5	1.3
			−86.9	(−62.2)		

[a]Values with counterpoise (CP) correction are given in italic. [b]The two values correspond to the upper and lower pair of bases, respectively (the sum is given in parentheses).

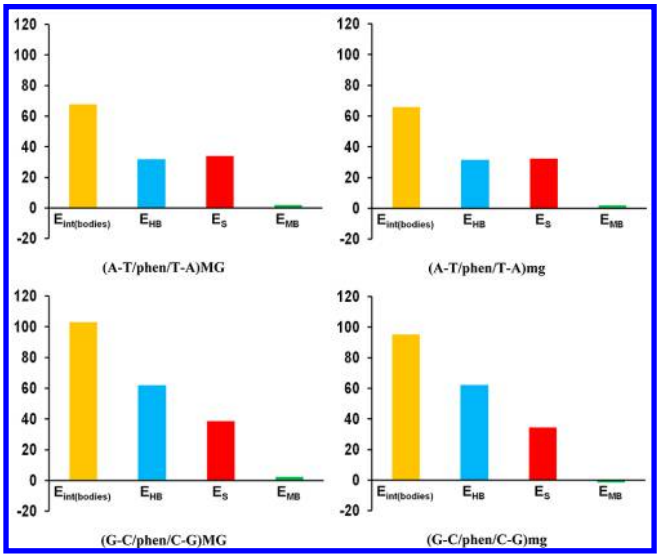

Figure 4. Trends in the partition of $-E_{int(bodies)}$ in the two-body and many-body terms at the M06-2X/6-31+G(d,p) level of calculation (in kcal mol^{-1}) for the studied systems with phen (the sign of the energy was specifically changed to give a better view).

an exception for the (A−T/phen/T−A)mg system, in which there is a difference of 1 kcal mol^{-1} between the upper and the lower base pair, with the smaller value of E_{HB} corresponding to the base pair with the extruded adenine (lower base pair). It must be mentioned that for this base pair the N···H−N hydrogen bond was weakened (Table 1). The values of E_{HB} in parentheses in Table 3 and in the trends in Figure 4 correspond to the sum of the values of E_{HB} for upper and lower base pairs. For the same system, there is almost no change in E_{HB} values when phen is introduced; thus, we can say that, in principle, intercalation does not affect the hydrogen bonds between the bases. However, as seen in the previous geometric parameter section, intercalation changes the distances and strength of the hydrogen bonds, but there are compensations of strengthening and weakening that would give a null balance of energy, and the E_{HB} before and after intercalation is very similar. Also, no significant difference is observed for E_{HB} between intercalation from the major groove and that from the minor groove (0.2 kcal mol^{-1} for the intercalation in A−T/T−A systems and also 0.2 kcal mol^{-1} for the intercalation in G−C/C−G systems). E_{HB} is always lower (in absolute value) for systems with adenine and thymine than it is for systems with guanine and cytosine (∼30 kcal mol^{-1}), which is not surprising because these systems have one more hydrogen bond.

The E_S values are more negative than those of E_f, as they do not contain the energy for the geometry distortion. As mentioned before, for systems without phen, the interstrand terms are usually repulsive, whereas the intrastrand terms are attractive and introduction of phen leads to all contributions to E_S being attractive. For this reason, E_S is always more negative in systems with phen (8−13 kcal mol^{-1} more negative; Table 3). These E_S values are also more negative for systems in which the intercalation takes place from the major groove (Table 3), and E_S is also more negative for systems with guanine and cytosine than it is for systems with adenine and thymine.

A comparison between E_{HB} and E_S shows that E_{HB} is always more important than E_S for systems with guanine and cytosine, whereas for systems with adenine and thymine, E_S becomes closer to E_{HB}. Intercalation leads to no special changes in E_{HB} because of the compensations between strengthening and weakening of the hydrogen bonds, whereas E_S becomes more negative and the stacking becomes a more important force because all terms are attractive in systems with phen. Thus, for systems with adenine and thymine, with only two hydrogen bonds, the stacking forces become an alternative to hydrogen bonding, whereas they cannot compete in guanine and cytosine systems with three hydrogen bonds.

Finally, the many-body interaction terms are small when compared to the two-body terms and can be cooperative ($E_{MB} < 0$) or anticooperative ($E_{MB} > 0$). Nevertheless, it is worth mentioning that for the systems in which intercalation takes place from the major groove, (A−T/phen/T−A)MG and (G−C/phen/C−G)MG, the values are quite high and always cooperative (−1.88 and −2.46 kcal mol^{-1}, respectively).

The energy of the interaction between the rigid fragments can be decomposed by the EDA into several contributions

$$\Delta E_{int} = \Delta E_{elstat} + \Delta E_{Pauli} + \Delta E_{orb} (+ \Delta E_{disp}) \quad (1)$$

where the electrostatic term ΔE_{elstat} corresponds to the classical electrostatic interaction between the unperturbed charge distributions of the rigid fragments, ΔE_{Pauli} comprises the destabilizing interactions between occupied orbitals, and the orbital interaction contribution, ΔE_{orb}, accounts for charge transfer and polarization terms. In the Computational Methods

DOI: 10.1021/ct5006104
J. Chem. Theory Comput. 2015, 11, 2714−2728

Table 4. Energy Decomposition Analysis (kcal mol^{-1}) between Phen and the Two Pairs of Bases at the M06-2X/TZP, M06-L/TZP, and B3LYP-D3/TZP Levels of Calculation

structures	contribution	M06-2X	M06-L	B3LYP-D3
(A−T/phen/T−A)MG	ΔE_{Pauli}	19.4	11.2	60.5
	ΔE_{elstat}	−27.2	−20.0	−29.0
	ΔE_{orb}	−16.2	−14.8	−12.6
	ΔE_{disp}			−49.4
	ΔE_{int}	−24.0	−23.6	−30.4 (−32.0)[a]
(A−T/phen/T−A)mg	ΔE_{Pauli}	18.2	10.1	55.3
	ΔE_{elstat}	−24.4	−17.6	−25.8
	ΔE_{orb}	−13.7	−14.3	−12.4
	ΔE_{disp}			−46.3
	ΔE_{int}	−19.9	−21.8	−29.2 (−29.4)[a]
(G−C/phen/C−G)MG	ΔE_{Pauli}	21.3	12.9	61.4
	ΔE_{elstat}	−31.7	−23.8	−33.0
	ΔE_{orb}	−17.8	−16.5	−14.3
	ΔE_{disp}			−48.7
	ΔE_{int}	−28.2	−27.4	−34.6 (−35.3)[a]
(G−C/phen/C−G)mg	ΔE_{Pauli}	16.8	9.2	56.4
	ΔE_{elstat}	−23.7	−17.3	−25.5
	ΔE_{orb}	−15.9	−13.3	−11.4
	ΔE_{disp}			−48.6
	ΔE_{int}	−22.8	−21.4	−28.8 (−29.4)[a]

[a]Values in parentheses are the values of ΔE_{int} at MP2/6-31G*(0.25) after removing the BSSE.

section, we mentioned that this EDA provides another interpretation of the energy terms, and it was carried out with the ADF program[70−72] using different functionals. As suggested by von Hopffgarten and Frenking[74] and observed by Acosta-Silva et al.,[60] if an explicit correction term for dispersion interactions is employed, then the EDA results remain unchanged and the dispersion correction appears as an extra term, ΔE_{disp}. On the contrary, if the dispersion interaction is part of the functional, then it will change the EDA results by weakening Pauli repulsion.

Table 4 presents the EDA for each intercalated system, whereas Figure 5 shows a cumulative bar diagram for the results obtained with the B3LYP-D3 functional in order to visualize better the trends for the systems with the intercalator. Whereas ΔE_{orb} terms are comparable for all functionals, the ΔE_{elstat} term is similar for M06-2X and B3LYP-D3, but it is less negative for the M06-L functional. On the other hand, the ΔE_{Pauli} term is greater in the B3LYP-D3 functional with the explicit term for dispersion, but it is nearly compensated by the R^{-6} term, with the resulting energy being 11.1, 9.0, 12.7, and 7.8 kcal mol^{-1} for the (A−T/phen/T−A)MG, (A−T/phen/T−A)mg, (G−C/phen/C−G)MG, and (G−C/phen/C−G)mg systems, respectively, after adding the ΔE_{Pauli} and ΔE_{disp} terms with opposite sign (Figure 5). These final values are comparable to the values of ΔE_{Pauli} obtained with functionals without an explicit term for dispersion, especially for M06-L. Moreover, interesting trends are observed in the attractive interactions of the EDA contributions within the four systems, calculated with the B3LYP-D3 functional for which an additional term for dispersion, ΔE_{disp}, is included. On one hand, ΔE_{disp} ranges from −46.3 for (A−T/phen/T−A)mg, with the extruded adenine, to −49.4 kcal mol^{-1} for (A−T/phen/T−A)MG. This small difference of 3.1 kcal mol^{-1} indicates a very similar contribution of ΔE_{disp} in the four systems. On the other hand, ΔE_{orb} varies by only 2.9 kcal mol^{-1}, from −11.4 to −14.3 kcal mol^{-1}, reflecting very close values of ΔE_{orb}. Finally, the values of ΔE_{elstat} go from −25.3 to −33.0 kcal mol^{-1}, spanning a difference of 7.7 kcal mol^{-1}. This appreciable difference means that this ΔE_{elstat} term will have a determining influence in the energy balance. If we quantify the attractive contributions of ΔE_{int} (B3LYP-D3 functional), then we see that the contribution of ΔE_{disp} goes from 50 to 55%, ΔE_{elstat} goes from 30 to 35%, and ΔE_{orb} is about 15%. These percentages show, in agreement with previous observations,[28,29,31,32,35,40,41] that the dispersion term is the most important contributor to the interaction of intercalators with DNA base pairs. Nevertheless, even with it being the most important attractive contribution, it is not enough to compensate the Pauli repulsion term. Dispersion forces are necessary but not sufficient to achieve stabilization in an intercalation process. Therefore, the roles of ΔE_{orb}, which is mainly related to charge transfer, and, especially, ΔE_{elstat}, which corresponds to the classical electrostatic interaction and has an important attractive

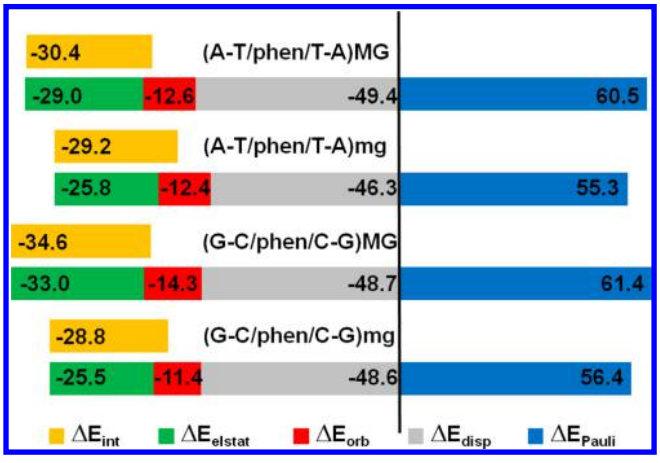

Figure 5. Cumulative bar diagram of the different contributions in the EDA at the B3LYP-D3/TZP level. Bars proportional to the value of ΔE_{int} are included close to the ΔE_{elstat} contribution to appreciate better the fitting of ΔE_{elstat} to ΔE_{int} (energy contributions in kcal mol^{-1}).

DOI: 10.1021/ct5006104
J. Chem. Theory Comput. 2015, 11, 2714−2728

contribution, become crucial to compensate ΔE_{Pauli} and make intercalation favorable. In fact, the values of ΔE_{elstat} are roughly similar to the values of ΔE_{int} (Table 4 and Figure 5), in agreement with a previous study on the role of electrostatics in stacked DNA base pairs, which showed that the electrostatic component of the stacking interaction closely fit the total interaction energy.[90]

The ΔE_{elstat} contribution (−33.0 kcal mol^{-1}) could be related to the stabilization of the system when intercalation takes place from the major groove for the systems with guanine and cytosine (see ΔE_{int} in Table 4). Indeed, ΔE_{disp} and ΔE_{orb} contributions do not change significantly when comparing (G−C/phen/C−G)MG to (G−C/phen/C−G)mg, with the ΔE_{elstat} being the most important in the (G−C/phen/C−G)MG system. This result would be in agreement with the fact that the electrostatic contribution to the interaction is closely related to the orientation of the interacting fragments, as observed by Řeha et al.[29] Of course, it should be kept in mind that we are analyzing the intrinsic nature of the interaction occurring inside the intercalation pocket between the intercalator and base pairs. In the case of metal complexes and real DNA, ancillary ligands would also play an important role by interacting with sugars, other bases, or phosphates of the duplex,[19,91] and we should take other nonintrinsic interactions into account to determine the selectivity for the major or minor groove. As recently found, the role of the water network surrounding the DNA in the stabilization of small-molecule binding to DNA also cannot be ignored.[92,93] Also very recently, Sasikala et al.[26] and Franco et al.[27] showed the importance of the steric factors and geometric restraints of the DNA, which will have a large contribution to the minor groove vs major groove preference in a real system, in their respective MD studies on intercalation/deintercalation.

Finally, concerning ΔE_{int}, all functionals, M06-2X, M06-L, and B3LYP-D3, give comparable trends, with the ΔE_{int} value corresponding to (G−C/phen/C−G)MG being the highest one, and those for (G−C/phen/C−G)mg and (A−T/phen/T−A)mg being the lowest. Moreover, the values obtained with the functionals with intrinsic dispersion correction are all very similar and are slightly lower than those obtained with B3LYP-D3 (extrinsic dispersion correction). We also calculated ΔE_{int} at the MP2/6-31*(0.25) level. The values, after removing the BSSE (Table 4), are almost the same as those reported with B3LYP-D3, thus confirming that the trends for ΔE_{int} are reliable.

In order to see the effect of the DNA backbone, we also carried out EDA at the B3LYP-D3/TZP level for the bb(G−C/phen/C−G)MG and bb(G−C/phen/C−G)mg systems. The results are depicted in Table 5.

Comparing the values in Tables 4 and 5, we see that the inclusion of the DNA backbone affects all of the attractive terms of the interaction: ΔE_{disp} contributions increased slightly, ΔE_{orb} increases notably, and ΔE_{elstat} does not change appreciably for the bb(G−C/phen/C−G)MG system, but it is more negative for the bb(G−C/phen/C−G)mg system than for the (G−C/phen/C−G)mg system. ΔE_{disp} still remains the dominant attractive term, but the repulsive ΔE_{Pauli} contribution is substantially increased. Consequently, this ΔE_{Pauli} repulsive contribution is always the dominant term, and no attractive term alone can balance the ΔE_{Pauli} contribution. Thus, the inclusion of the DNA backbone influences all of the energetic terms of the EDA. Nevertheless, when putting all of the terms together, the main conclusion obtained above for the systems without the DNA backbone remains: dispersion forces are necessary for the intercalation, but they are not enough to balance the Pauli repulsion and charge transfer contributions, and electrostatic forces are fundamental to stabilize the intercalator between base pairs in the DNA intercalation step.

Table 5. Energy Decomposition Analysis (kcal mol^{-1}) for the bb(G−C/phen/C−G)MG and bb(G−C/phen/C−G)mg Systems Including Sugars and Phosphates at the B3LYP-D3/TZP Level of Calculation

structures	contribution	B3LYP-D3
bb(G−C/phen/C−G)MG	ΔE_{Pauli}	78.8
	ΔE_{elstat}	−31.7
	ΔE_{orb}	−21.7
	ΔE_{disp}	−49.8
	ΔE_{int}	−24.3
bb(G−C/phen/C−G)mg	ΔE_{Pauli}	80.0
	ΔE_{elstat}	−31.4
	ΔE_{orb}	−18.1
	ΔE_{disp}	−51.3
	ΔE_{int}	−20.8

Interaction Properties. The trends observed in the interaction of phen with stacked base pairs can be analyzed in terms of the electronic structure of the base pair/phen/base pair model systems using polarizability, dipolar moments, molecular electrostatic potentials (MEPs), electronic density, charges, and frontier molecular orbitals (MOs).

Table 6 presents one-electron properties (dipole moment and polarizability) of the studied systems. The high value of μ for phen (3.3 D) and base pairs (1.5 D for A−T and, especially, 6.1 D for G−C) accounts for the important role of the electrostatic contribution in the intercalation process, in agreement with the EDA results described above. With respect to the importance of the electrostatic contribution, it must be said that, as a general trend, the stacked systems with phen display better electrostatic complementarity, and thus stronger electrostatic attraction, than the stacked systems without phen (a more extended explanation regarding the MEPs is described in the Supporting Information). The polarizability (α) also gives information about the electron distribution, since it depends on the relative tendency of a charge distribution, such as the electron cloud of a molecule, to be distorted from its normal shape by an external electric field. The quite large values of α for phen (152.7 au^{-3}), base pairs (170.3 au^{-3} for A−T and 170.5 au^{-3} for G−C), and stacked base pairs (332.9 au^{-3} for A−T/T−A and 324.0 au^{-3} G−C/C−G) emphasize the importance of dispersion forces in the intercalation, also in agreement with the important role of dispersion forces found in the EDA.

Analysis of the energies of the frontier MOs (see Table 6 and Figure S2 of the Supporting Information) suggests that phen should be a better electron acceptor than any of the stacked base pairs. Indeed, phen has the LUMO lying at −0.03123 au, which is more negative than any of the LUMOs of the stacked base pairs (−0.00788 au for A−T/T−A and −0.01271 au for G−C/C−G). Thus, stacked base pairs would act as electron donors in the interaction with phen, as confirmed by the energies of the HOMO (−0.27540 au for A−T/T−A and −0.24452 au for G−C/C−G, which are higher in energy than the HOMO of phen, −0.28519 au). Thus, the interaction between phen and base pairs might also be stabilized by some charge transfer (CT) contribution.

DOI: 10.1021/ct5006104
J. Chem. Theory Comput. 2015, 11, 2714−2728

Table 6. One-Electron Properties and Energies of Frontier Molecular Orbitals of the Analyzed Systems

system	HOMO[a]	LUMO[b]	μ^c	α^d
phen	−0.28519 (−7.76)	−0.03123 (−0.85)	3.3	152.7
A−T	−0.27402 (−7.46)	−0.01087 (−0.30)	1.5	170.3
A−T/T−A	−0.27540 (−7.49)	−0.00788 (−0.21)	0.6	332.9
(A−T/phen/T−A)MG	−0.25985 (−7.07)	−0.02439 (−0.66)	3.8	460.7
(A−T/phen/T−A)mg	−0.27268 (−7.42)	−0.03379 (−0.92)	2.3	461.9
G−C	−0.24550 (−6.68)	−0.02213 (−0.60)	6.1	170.5
G−C/C−G	−0.24452 (−6.65)	−0.01271 (−0.34)	3.3	324.0
(G−C/phen/C−G)MG	−0.24812 (−6.75)	−0.02943 (−0.80)	1.8	459.9
(G−C/phen/C−G)mg	−0.24304 (−6.61)	−0.02670 (−0.73)	0.6	456.9

[a]Energy of HOMO in au (eV in parentheses). [b]Energy of LUMO in au (eV in parentheses). [c]Dipole moment in debye. [d]Polarizability in au^{-3}.

It is known that CT plays an important role in organic and biological $\pi-\pi$ complex formation.[94] Some examples can be found in the experimental work of Kelly et al.,[95−97] which addresses the intercalation of $[Ru(TAP)_2(dppz)]^{2+}$ in DNA. In the lowest excited state, the Ru complex is able to oxidize guanine-containing polynucleotides via CT from guanine-rich nucleotides to the intercalator in a mechanism consistent with a proton-coupled electron transfer process. Moreover, such CT from nucleotides to the intercalated complex in an excited state has been discussed very recently from a theoretical point of view by Monari et al.,[98−101] who have provided new insight on the nature the process. However, when the complex is in the ground state, the magnitude of real electron transfer is usually small.[102] According to Mulliken's CT theory, the formation of $\pi-\pi$ CT complexes requires the maximum overlap and minimum energy gap between the HOMO of the donors and the LUMO of the acceptors.[103] In our study, energy gaps between the HOMO of stacked base pairs and the LUMO of phen are 6.6 and 5.8 eV for A−T/T−A and G−C/C−G, respectively. Thus, we find quite high energy gaps between the HOMOs of stacked base pairs and the LUMO of phen, suggesting a small extent of CT. The frontier orbitals of all systems with intercalated phen, however, have an important contribution from both fragments, phen and base pair MOs, as shown in Figure 6 for (A−T/phen/T−A)MG and its constituents and in Figure S2 of the Supporting Information for all of the studied systems.

Nevertheless, minor perturbations of the energies of the frontier orbitals associated with HOMO and LUMO of isolated phen are observed in the intercalation complex. These orbitals would also correspond to the HOMO and LUMO orbitals of the intercalated systems containing adenine and thymine in which some contribution of the base pairs is found. The energy gaps of 6.4 and 6.5 eV for (A−T/phen/T−A)MG and (A−T/phen/T−A)mg, respectively, are similar to the HOMO − LUMO energy gap of the isolated phen (6.9 eV). On the other hand, for G−C/C−G systems, only few frontier orbitals have both phen and base pair contributions. The orbitals associated with the HOMO and LUMO of the isolated phen are the HOMO − 2 and LUMO of (G−C/phen/C−G)MG and (G−C/phen/C−G)mg, respectively. The energy gaps of 6.7 and 6.6 eV, are, again, similar to that of isolated phen (6.9 eV). Therefore, minor perturbations of the energies and the nature of the orbitals associated with phen were observed upon intercalation, suggesting that the effect of the electron-transfer stabilization is not the major contribution to the $\pi-\pi$ stacking interaction between phen and the base pairs. This result would be in agreement with the results of the EDA, which gave, roughly, only 15% of the attractive contribution to the

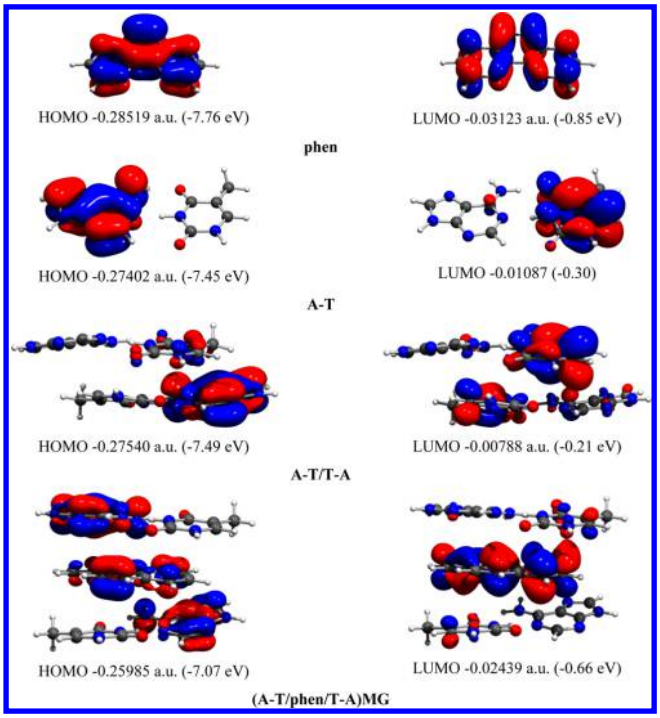

Figure 6. HOMO and LUMO MOs for the phen intercalator, A−T base pairs, the stacked systems without phen A−T/T−A, and intercalating phen from the major groove (A−T/phen/T−A)MG at the M06-2X/6-31+G(d,p) level of theory.

intercalation arising from the ΔE_{orb} contribution associated with charge transfer. In fact, the π electron charge transfer assigned to the intercalation process ranges from 0.0227 for (A−T/phen/T−A)mg to 0.0434 for (G−C/phen/C−G)mg, as will be discussed in the next paragraph.

The charge is redistributed through the systems when intercalation takes place. As recommended by Šponer et al.,[64] charges were obtained by means of the NBO analysis[65,66] and are presented in Table 7 for each base, phen, and their associations. In all intercalated systems, we find that phen accumulates negative charge, although this π charge transfer is very small (from −0.0227 to −0.0434), as expected from the orbital analysis and EDA. On the other hand, we observe that the σ electron transfer is similar to the stacked systems without phen.[59,60] That is, for A−T/T−A, the electron transfer goes from purine to pyrimidine bases, whereas for the systems with G−C/C−G, the opposite behavior is observed, and σ electron transfer goes from pyrimidine to purine bases. Again, this σ electron transfer through hydrogen bonding can be explained, in the case of systems with adenine and thymine, by the

DOI: 10.1021/ct5006104
J. Chem. Theory Comput. 2015, 11, 2714−2728

Table 7. Distribution of the NPA Charges on Purine and Pyrimidine DNA Bases and Phen Intercalator for the Four Stacked Systems Containing Phen[a]

structures	Q_{Purine}	$Q_{Pyrimidine}$	$Q_{Phenanthroline}$
A−T/T−A	0.0477/0.0514	−0.0403/−0.0589	
(A−T/phen/T−A)MG	0.0680/0.0644	−0.0478/−0.0503	−0.0343
(A−T/phen/A−T)mg	0.0557/0.0419	−0.0432/−0.0318	−0.0227
G−C/C−G	−0.0362/−0.0355	0.0362/0.0356	
(G−C/phen/C−G)MG	−0.0319/−0.0346	0.0547/0.0532	−0.0414
(G−C/phen/C−G)mg	−0.0151/−0.0162	0.0367/0.0380	−0.0434

[a]The distribution of charge for the stacked systems without phen is also shown for comparison.

stronger N−H···N hydrogen bond, which will lead to the electron transfer from adenine to thymine. In fact, the differences on the charge values between the upper (Q_{Purine} = 0.0557 and $Q_{Pyrimidine}$ = −0.0432) and lower base pairs (Q_{Purine} = 0.0419 and $Q_{Pyrimidine}$ = −0.0318) in the extruded system (A−T/phen/T−A)mg can be attributed to the weaker N···H−N hydrogen bond in the lower base pair owing to the dislocation of adenine. On the other hand, for the G−C/C−G systems, because only the O···H−N hydrogen bond transfers σ charge from guanine to cytosine, but the other two N−H···O and N−H···N hydrogen bonds contribute to a σ transfer on the opposite direction, the global σ charge transfer is from pyrimidine base to purine base. These trends in σ charge transfer are also supported by the AIM analysis, as we shall see in the next paragraph.

Indeed, we can obtain more insight regarding the behavior of these hydrogen bonds and the other weak interactions by analyzing the topological properties of the electron density[68] using the AIM theory of Bader et al.[68,104,105] Figure S3 of the Supporting Information shows the topologies of each intercalated system, whereas Tables S1−S4, Supporting Information, present values for the electronic density (ρ) and its laplacian ($\nabla^2\rho$) at each bond critical point (BCP) of the weak interactions. The values of ρ at BCPs corresponding to N_6−H···O_4 hydrogen bonds decrease from 0.0233 au/0.0264 au in A−T/T−A to 0.0226 au/0.0226 au in (A−T/phen/T−A)MG, in agreement with the increase of the distances in N_6−H···O_4 hydrogen bonds. Moreover, these values of 0.0226 au/0.0226 au are lower than the values of 0.0500 au/0.0498 au found at N_1···H−N_3 hydrogen bonds, also in (A−T/phen/T−A)MG, in agreement with the σ electron transfer from adenine to thymine. When intercalation takes place from the minor groove, there is a decrease of ρ at the BCP corresponding to the lower N_1···H−N_3 hydrogen bond, from 0.0456 to 0.0395 au, in agreement with the weakening of such a hydrogen bond. Also, the values of ρ at the N_1···H−N_3 hydrogen bonds are higher (0.0490 au/0.0395 au) than the ρ values found at N_6−H···O_4 hydrogen bonds (0.0260 au/0.0259 au), in agreement with the σ electron transfer from adenine to thymine. For all of the A−T/T−A systems, the values of ρ at each BCP of the hydrogen bonds are in agreement with the order of strength of the hydrogen bonds, with the N_1···H−N_3 hydrogen bond being stronger than the N_6−H···O_4 hydrogen bond, which is much stronger than the C_2−H···O_2 hydrogen bond (Tables 1, S1, and S2). On the other hand, for the G−C/C−G systems, when intercalation takes place from the major groove, there is an increase of ρ at the BCPs corresponding to O_6···H−N_4 hydrogen bonds (from 0.0304 au/0.0302 au to 0.0320 au/0.0320 au) and N_1−H···N_3 hydrogen bonds (from 0.0333 au/0.0333 au to 0.0356 au/0.0351 au), in agreement with the strengthening of these two hydrogen bonds observed before. These last values of 0.0356 au/0.0351 au for N_1−H···N_3 hydrogen bonds along with the values of 0.0299 au/0.0299 au for N_2−H···O_2 hydrogen bonds will determine the direction of the σ electron transfer from cytosine to guanine since the values of ρ found at the O_6···H−N_4 hydrogen bonds (0.0320 au/0.0320 au) are not large enough to reverse the direction of the σ charge transfer. When intercalation takes place from the minor groove, there is a decrease of the ρ value, from 0.0294 au/0.0297 au to 0.0254 au/0.0255 au at the BCP, corresponding to the N_2−H···O_2 hydrogen bond, and an increase of ρ, from 0.0304 au/0.0302 au to 0.0378 au/0.0378 au at the BCP, corresponding to the O_6···H−N_4 hydrogen bond, whereas ρ at the BCP, corresponding to the N_1−H···N_3, has no significant change (from 0.0333 au/0.0333 au to 0.0335 au/0.0335 au); all of these trends are in agreement with a weakening of the N_2−H···O_2 hydrogen bond, a strengthening of the O_6···H−N_4 hydrogen bond, and no significant changes in N_1−H···N_3 hydrogen bonds. Also, in this case, the values for ρ at N_1−H···N_3 hydrogen bonds together with those at N_2−H···O_2 hydrogen bonds are higher than the values of ρ at the O_6···H−N_4 hydrogen bonds. These trends are in agreement with the above observed σ electron transfer from cytosine to guanine. All of these results corroborate the important influence of intercalation on hydrogen bonds.

Topological analysis also revealed evidence of π-stacking interactions. As shown by Hobza et al.,[45] these interactions are weak, with a very small value of ρ at the BCPs associated with π-stacking interactions. Such values ranged from 0.0058 to 0.0087 au at the 16 BCPs of the (A−T/phen/T−A)MG system, from 0.0038 to 0.0086 au at the 14 BCPs of the (A−T/phen/T−A)mg system, from 0.0054 to 0.0090 au at the 15 BCPs of the (G−C/phen/C−G)MG system, and from 0.0042 to 0.0087 au at the 14 BCPs of the (G−C/phen/C−G)mg system, which are common values of ρ at BCPs involved in π-stacking interactions.[106] All values of $\nabla^2\rho$ at each BCP were positive, as expected for closed-shell interactions. These π-stacking interactions were also characterized in terms of CCPs (see Figure S3 of the Supporting Information), as was done by Zhikol et al.,[107] and 12, 11, 9, and 10 CCPs were found for the (A−T/phen/T−A)MG, (A−T/phen/T−A)mg, (G−C/phen/C−G)MG, and (G−C/phen/C−G)mg systems, respectively, with ρ values between 0.0020 and 0.0056 au along with positive values for the Laplacian.

CH_3−π interactions are also present in the systems with adenine and thymine. For the (A−T/phen/T−A)MG system, one bond path (BP) associated with the CH_3(Td)···C_4(phen) BCP is characterized by ρ of 0.0067 au and a positive Laplacian, whereas for (A−T/phen/T−A)mg, one BP associated with the CH_3(Td)···C_8(phen) BCP is found between the lower thymine and phen, with ρ of 0.0064 au and a positive Laplacian (Tables S1 and S2 and Figure S3 of the Supporting Information). For

DOI: 10.1021/ct5006104
J. Chem. Theory Comput. 2015, 11, 2714−2728

the (A−T/phen/T−A)mg system, it is also worth mentioning the BP associated with CH_3(Tu)···N_9(Ad) BCP with a ρ value of 0.0016 au and a positive Laplacian (see Table S2 and Figure S3 of the Supporting Information). Figures 2 and S3 show the displacement of adenine to allow this stabilizing interaction. The importance of stabilizing CH/π interactions has been already stressed for methane/adenine systems.[108]

Further Comments. After the EDA and taking into account the results of polarizability, dipolar moment, electronic density, charge transfer, MEPs, and the analysis of frontier orbitals, the nature of the interaction can be mainly assigned to the dispersion forces, in agreement with other studies with several intercalators.[28,29,31,32,35,40,41] Nevertheless, dispersion forces are necessary but not sufficient to compensate the Pauli repulsion between electrons of two fragments with the same spin and therefore charge transfer contribution and the electrostatic interactions, in particular, become important to achieve stabilization in the intercalation process. This important role of the electrostatic contribution is evidenced not only from the EDA and the dipolar moments but also from the MEP maps, since, in the final orientation, all systems tried to avoid electrostatic repulsions with the exception of (A−T/phen/T−A)mg, for which a CH_3−π attractive interaction appears to compensate. The contribution of the charge transfer in the interaction of phen with base pairs is the smallest term, as evidenced in the EDA, NPA, and AIM analysis. Nevertheless, such a contribution becomes more important, and non-negligible, when the DNA backbone is included in the model. The direction of π charge transfer, however, is, in all cases, in agreement with the nature of the intercalators (electron acceptors) and base pairs (electron donors), whereas the sense of σ charge transfer is from purines to pyrimidines in systems with adenine and thymine and from pyrimidines to purines for systems with guanine and cytosine.

This work follows the publication of two recent reviews on intercalation processes[12,13] and the works of Sasikala et al.[26] and Franco et al.,[27] based on molecular dynamics simulations, on the process of intercalation/deintercalation of different small molecules in DNA, reflecting some current debate in the literature on these processes. They show that groove binding occurs prior to intercalation in the global process. Such groove binding occurs very fast (tenths of a millisecond) compared to intercalation (in the range of few milliseconds). Moreover, entropy and the desolvation energy are shown to play a major role in the kinetics of the process. Since the cytotoxic effect of any intercalator depends on the time of residence of the drug between base pairs,[109] as indicated by Sasikala et al.,[26] the design of an efficient drug should aim at an increased drug−DNA stacking interactions to stabilize the intercalated state, but it should do so at a less stable groove binding state to make the kinetics faster. We suggest that once the intrinsic contributions to interaction energy are quantified and understood in the present work, it is possible to modulate them by the introduction of different substituents in the intercalator. Thus, derivatization of any intercalator, phen in our case, by substitution in number and position, with groups that are able to tune the intrinsic terms ruling intercalation could be a good strategy for drug design. In fact, such an effect of substitution in number and position on cytotoxicity was observed for methylation of phen[15] in positions 4-, 5-, 4,7-, 5,6-, and 3,4,7,8-, with the 5,6-Mephen derivative being the most cytotoxic system, whereas neither 4-Mephen nor the 4,7-Mephen derivative were cytotoxic. After the previous analysis, we believe that the intrinsic forces governing intercalation could play an important role in favoring intercalation over groove binding in some derivatives and thus in the discrimination of cytotoxic derivatives. Of course, many variables govern the process of intercalation/deintercalation of small molecules in DNA, namely, aside from the intrinsic forces studied here, solvation effects, entropy, and steric effects, as suggested by Sasikala et al.[26] and Franco et al.[27] Even interactions of ancillary ligands with DNA could also play some important role in the process. Nevertheless, intrinsic interactions that take place directly in the intercalation pocket must have a primary role, and their comprehension and rationalization become fundamental.

Thus, because our study aimed at giving new and very detailed insight on the nature of the intrinsic interactions that govern intercalation (ΔE_{disp}, ΔE_{elstat}, ΔE_{orb}, and ΔE_{Pauli}), we used a model that could be treated at the QM level with our technical resources (two base pairs of DNA and the intercalator). Such intrinsic interactions were studied previously in the seminal works of Bondarev et al.[28] and Řeha et al.[29] with three-body models (intercalator + one base pair), which continued to be used for more than 1 decade[28−34] until the recent work of Hazarika et al.[33] Nevertheless, as indicated by Hill et al.,[37] we need the other base pair to provide a better description of the role of the intrinsic forces that govern intercalation. On the other hand, when two base pairs are considered,[35−41] either no analysis of the intrinsic interactions is carried out or the main conclusion is that dispersion and the electrostatic contributions are more important than charge transfer. However, Pauli repulsion is not taken into account. In the EDA carried out in our work, we observed that, in fact, the Pauli repulsion contribution is always the dominant term and it cannot be balanced by any attractive contribution alone. We analyzed the inclusion of the DNA backbone in the (G−C/phen/C−G)MG and (G−C/phen/C−G)mg systems by adding the sugars and phosphates surrounding the intercalation pocket (bb(G−C/phen/C−G)MG and bb(G−C/phen/C−G)mg systems. We optimized such structures by using the recently developed PM6-DH2 semiempirical method that includes dispersion effects.[82] As indicated previously, PM6-DH2 has been found to give quite good performance for stacking interactions[85] and gave optimized geometries comparable to those with DFT-D methods for the (A−T/phen/T−A)MG, (A−T/phen/T−A)mg, (G−C/phen/C−G)MG, and (G−C/phen/C−G)mg systems without sugars and phosphates.[86] Moreover, it must be said that examples of the application of PM6-DH2 in DNA systems are scarce in the literature. Looking at the studied geometrical parameters when the DNA backbone is included (Table 2), no significant changes are observed when comparing the (G−C/phen/C−G)MG and (G−C/phen/C−G)mg systems without including the DNA backbone to the bb(G−C/phen/C−G)MG and bb(G−C/phen/C−G)mg systems including sugars and phosphates. We also carried out EDA analysis for the optimized bb(G−C/phen/C−G)MG and bb(G−C/phen/C−G)mg systems at the B3LYP-D3/TZP level, and, although the individual values of ΔE_{disp}, ΔE_{elstat}, ΔE_{orb}, and ΔE_{Pauli} are modified, the same global conclusion given in the beginning of this section is obtained when including the DNA backbone in the EDA; additionally, even the role of the ΔE_{orb} term is increased in its importance.

Finally, it must be said that our model has been simulated under anhydrous conditions, but, as pointed out by Šponer et

DOI: 10.1021/ct5006104
J. Chem. Theory Comput. 2015, 11, 2714−2728

al.,[64] gas-phase calculations reveal the intrinsic interactions in the studied systems with no perturbation by external effects, and, at first glance, they may appear to be rather far away from physiological systems. However, one needs to interpret the intrinsic molecular interactions correctly, as this knowledge constitutes an important prerequisite toward understanding the role of intercalators between nucleobases in DNA structure and the evaluation of the role of different intrinsic contributions that govern the intercalation interaction. Moreover, such knowledge of the intrinsic interactions may also be used for the development of force fields.

Thus, once the intrinsic nature of the interaction is understood and quantified and by taking into account that any drug should be designed with high polarizability and dipole moment to increase its interaction with DNA,[110] it is possible to functionalize phen with groups that produce changes along those lines. This will be one of the aims of a forthcoming paper.[86]

CONCLUSIONS

We carried out complete DFT optimizations on stacked systems, A−T/T−A and G−C/C−G, incorporating phenanthroline intercalator by using different functionals that take into account dispersion forces in order to study how the intercalation of phen affects the structure, energetics, and bond properties of the DNA base pairs. In our study, intercalation can take place from the major groove, from the minor groove, or between adenine and thymine or guanine and cytosine base pairs, affording different structures and energies. For instance, intercalation from the minor groove in adenine−thymine systems leads to one adenine being extruded from the stacking. This was never observed in guanine−cytosine pairs. Also, as a general trend, there is an opening of the θ twist angle in all of the studied systems with the exception of the (G−C/phen/C−G)mg system, for which θ does not change appreciably. Moreover, a relationship between intercalation and hydrogen bonding was found.

Multi-body energy analysis shows that the E_{HB} component does not change appreciably when intercalation takes place because of the compensation between strengthening and weakening of the different hydrogen bonds, whereas E_S becomes appreciably more negative and the stacking becomes a more important force because all terms are attractive. On the other hand, the EDA leads us to conclude that the dispersion contribution is necessary for the intercalation process but not sufficient to to compensate the Pauli repulsion term, ΔE_{Pauli}, and that the orbital contribution, ΔE_{orb}, and, especially, the electrostatic contribution, ΔE_{elstat}, become crucial for the final stabilization of the intercalation process. On the basis of these results, it seems likely that functionalization of phen may allow the intercalation energy and its effectiveness as a drug to be enhanced. With these results in mind, we shall undertake some theoretical studies of the intercalation of phen derivatives to provide more insight into the influence of the substituents on the intercalation process in DNA. These studies will be the subject of a forthcoming paper.[86] We hope that our work will help to shed some light on such important processes of current interest.

ASSOCIATED CONTENT

Supporting Information

Discussion on the electrostatic potential maps of the studied systems, frontier orbitals from HOMO − 5 to LUMO + 5, AIM topologies, values of the electron density (ρ) and Laplacian ($\nabla^2\rho$) of all BCPs corresponding to weak interactions found in (A−T/phen/T−A)MG, (A−T/phen/T−A)mg, (G−C/phen/C−G)MG, and (G−C/phen/C−G)mg systems, and Cartesian coordinates of the optimized structures. The Supporting Information is available free of charge on the ACS Publications website at DOI: 10.1021/ct5006104.

AUTHOR INFORMATION

Corresponding Authors

*(A.G.) E-mail: agmestres@fc.ul.pt.
*(M.J.C.) E-mail: mjcalhorda@ciencias.ulisboa.pt.

Funding

This research was financially supported by the Fundação para a Ciência e a Tecnologia (FCT) by means of postdoctoral grant SFRH/BPD/89722/2012 to A.G., the program "Ciência 2008", and grant UID/MULTI/00612/2013.

Notes

The authors declare no competing financial interest.

ACKNOWLEDGMENTS

Luis Filipe Veiros, Pedro D. Vaz, Nuno A. G. Bandeira, and Ángel Sánchez González are acknowledged for fruitful discussions.

DEDICATION

This paper is dedicated to the memory of Prof. Tom Ziegler (1945−2015).

REFERENCES

(1) Harrap, K. R. *Cancer Treat. Rev.* **1985**, *12*, 21−33.
(2) Bandarra, D.; Lopes, M.; Lopes, T.; Almeida, J.; Saraiva, M. S.; Dias, M. V.; Nunes, C. D.; Félix, V.; Brandão, P.; Vaz, P. D.; Meireles, M.; Calhorda, M. J. *J. Inorg. Biochem.* **2010**, *104*, 1171−1177.
(3) Ikotun, O. F.; Higbee, E. M.; Ouellette, W.; Doyle, R. P. *J. Inorg. Biochem.* **2009**, *103*, 1254−1264.
(4) Liang, X.; Zou, X.; Tan, L.; Zhu, W. *J. Inorg. Biochem.* **2010**, *104*, 1259−1266.
(5) Prasad, P.; Sasmal, P. K.; Majumdar, R.; Dighe, R. R.; Chakravarty, A. R. *Inorg. Chim. Acta* **2010**, *363*, 2743−2751.
(6) Seng, H.-L.; Von, S.-T.; Tan, K.-W.; Maah, M. J.; Ng, S.-W.; Rahman, R. N. Z. A.; Caracelli, I.; Ng, C.-H. *BioMetals* **2010**, *23*, 99−118.
(7) Riera, X.; Moreno, V.; Ciudad, C. J.; Noe, V.; Font-Bardia, M.; Solans, X. *Bioinorg. Chem. Appl.* **2007**, No. 98732.
(8) Xu, H.; Zheng, K. C.; Deng, H.; Lin, L. J.; Zhang, Q. L.; Ji, L. N. *New J. Chem.* **2003**, *27*, 1255−1263.
(9) Zeglis, B. M.; Pierre, V. C.; Barton, J. K. *Chem. Commun.* **2007**, *44*, 4565−4679.
(10) Liu, H. K.; Sadler, P. J. *Acc. Chem. Res.* **2011**, *44*, 349−359.
(11) Boer, D. R.; Canals, A.; Coll, M. *Dalton Trans.* **2009**, *3*, 399−414.
(12) Mukherjee, A.; Sasikala, W. D. *Adv. Protein Chem. Struct. Biol.* **2013**, *92*, 1−62.
(13) Vargiu, A. V.; Magistrato, A. *ChemMedChem* **2014**, *9*, 1966−1981.
(14) Grueso, E.; López-Pérez, G.; Castellano, M.; Prado-Gotor, R. *J. Inorg. Biochem.* **2012**, *106*, 1−9.
(15) Brodie, C. R.; Grant Collins, J.; Aldrich-Wright, J. R. *Dalton Trans.* **2004**, 1145−1152.
(16) Prasad, P.; Sasmal, P. K.; Majumdar, R.; Dighe, R. R.; Chakravarty, A. R. *Inorg. Chim. Acta* **2010**, *363*, 2743−2751.
(17) Hall, J. P.; O'Sullivan, K.; Naseer, A.; Smith, J. A.; Kelly, J. M.; Cardin, C. J. *Proc. Natl. Adad. Sci. U.S.A.* **2011**, *108*, 17610−17614.
(18) Neidle, S. *Nat. Chem.* **2012**, *4*, 594−595.

DOI: 10.1021/ct5006104
J. Chem. Theory Comput. 2015, 11, 2714−2728

(19) Song, H.; Kaiser, J. T.; Barton, J. K. *Nat. Chem.* **2012**, *4*, 615−620.
(20) Niyazi, H.; Hall, J. P.; O'Sullivan, K.; Winter, G.; Sorensen, T.; Kelly, J. M.; Cardin, C. J. *Nat. Chem.* **2012**, *4*, 621−628.
(21) Trieb, M.; Rauch, C.; Wibowo, F. R.; Wellenzohn, B.; Liedl, K. R. *Nucleic Acids Res.* **2004**, *32*, 4696−4703.
(22) Mukherjee, A.; Lavery, R.; Bagchi, B.; Hynes, J. T. *J. Am. Chem. Soc.* **2008**, *130*, 9747−9755.
(23) Robertazzi, A.; Vargiu, A. V.; Magistrato, A.; Ruggerone, P.; Carloni, P.; de Hoog, P.; Reedijk, J. *J. Phys. Chem. B* **2009**, *113*, 10881−10890.
(24) Vargiu, A. V.; Magistrato, A. *Inorg. Chem.* **2012**, *51*, 2046−2057.
(25) Galindo-Murillo, R.; Ruíz-Azuara, L.; Moreno-Esparza, R.; Cortés-Guzmán, F. *Phys. Chem. Chem. Phys.* **2012**, *14*, 15539−15546.
(26) Sasikala, W. D.; Mukherjee, A. *Phys. Chem. Chem. Phys.* **2013**, *15*, 6446−6455.
(27) Franco, D.; Vargiu, A. V.; Magistrato, A. *Inorg. Chem.* **2014**, *53*, 7999−8008.
(28) Bondarev, D. A.; Skawinski, W. J.; Venanzi, C. A. *J. Phys. Chem. B* **2000**, *104*, 815−822.
(29) Řeha, D.; Kabeláč, M.; Ryjaček, F.; Šponer, J.; Šponer, J. E.; Elstner, M.; Suhai, S.; Hobza, P. *J. Am. Chem. Soc.* **2002**, *124*, 3366−3376.
(30) Kumar, A.; Elstner, M.; Suhai, S. *Int. J. Quantum Chem.* **2003**, *95*, 44−59.
(31) El-Gogary, T. M.; Koehler, G. *J. Mol. Struct.: THEOCHEM* **2007**, *808*, 97−109.
(32) El-Gogary, T. M.; Koehler, G. *J. Mol. Struct.: THEOCHEM* **2009**, *895*, 57−64.
(33) Hazarika, P.; Bezharuah, B.; Das, P.; Medhi, O. K.; Medhi, C. *J. Biophys. Chem.* **2011**, *2*, 152−157.
(34) Li, S.; Cooper, V. R.; Thonhauser, T.; Lundqvist, B. I.; Langreth, D. C. *J. Phys. Chem. B* **2009**, *113*, 11166−11172.
(35) Xiao, X.; Antony, S.; Pommier, Y.; Cushman, M. *J. Med. Chem.* **2005**, *48*, 3231−3238.
(36) Langner, K. M.; Kedzierski, P.; Sokalski, W. A.; Leszczynski, J. *J. Phys. Chem. B* **2006**, *110*, 9720−9727.
(37) Hill, J. G.; Platts, J. A. *Chem. Phys. Lett.* **2009**, *479*, 279−283.
(38) Ambrosek, D.; Loos, P.-F.; Assfeld, X.; Daniel, C. *J. Inorg. Biochem.* **2010**, *104*, 893−901.
(39) Biancardi, A.; Biver, T.; Marini, A.; Mennucci, B.; Secco, F. *Phys. Chem. Chem. Phys.* **2011**, *13*, 12595−12602.
(40) Hohenstein, E. G.; Parrish, R. M.; Sherrill, C. D.; Turney, J. M.; Schaefer, H. F., III *J. Chem. Phys.* **2011**, *135*, 174107.
(41) Deepa, P.; Kolandaivel, P.; Senthilkumar, K. *Mater. Sci. Eng., C* **2012**, *32*, 423−431.
(42) Cordier, C.; Pierre, V. C.; Barton, J. K. *J. Am. Chem. Soc.* **2007**, *129*, 12287−12295.
(43) Zhao, Y.; Truhlar, D. G. *Acc. Chem. Res.* **2008**, *41*, 157−167.
(44) Zhao, Y.; Truhlar, D. G. *Theor. Chem. Acc.* **2008**, *120*, 215−241.
(45) Dabkowska, I.; Gonzalez, H. V.; Jurecka, P.; Hobza, P. *J. Phys. Chem. A* **2005**, *109*, 1131−1136.
(46) Dabkowska, I.; Jurecka, P.; Hobza, P. *J. Chem. Phys.* **2005**, *122*, 204322−1−9.
(47) Šponer, J.; Riley, K. E.; Hobza, P. *Phys. Chem. Chem. Phys.* **2008**, *10*, 2595−2610.
(48) Pitonák, M.; Janowski, T.; Neogrády, P.; Pulay, P.; Hobza, P. *J. Chem. Theory Comput.* **2009**, *5*, 1761−1766.
(49) Hargis, J. C.; Schaefer, H. F., III; Houk, K. N.; Wheeler, S. E. *J. Phys. Chem. A* **2010**, *114*, 2038−2044.
(50) Gu, J.; Wang, J.; Leszcynski, J.; Xie, Y.; Schaefer, H. F., III *Chem. Phys. Lett.* **2008**, *459*, 164−166.
(51) Gu, J.; Wang, J.; Leszcynski, J.; Xie, Y.; Schaefer, H. F., III *Chem. Phys. Lett.* **2009**, *473*, 209−210.
(52) Sherrill, C. D.; Takatani, T.; Hohenstein, E. G. *J. Phys. Chem. A* **2009**, *113*, 10146−10159.
(53) Steinmann, S. N.; Csonka, G.; Corminboeuf, C. *J. Chem. Theory Comput.* **2009**, *5*, 2950−2958.
(54) Hohenstein, E. G.; Chill, S. T.; Sherrill, C. D. *J. Chem. Theory Comput.* **2008**, *4*, 1996−2000.
(55) Valdes, H.; Spiwok, V.; Rezac, J.; Reha, D.; Abo-Riziq, A. G.; de Vries, M. S.; Hobza, P. *Chem.—Eur. J.* **2008**, *14*, 4886−4898.
(56) Zhao, Y.; Truhlar, D. G. *J. Phys. Chem. A* **2004**, *108*, 6908−6918.
(57) Hehre, W. J.; Radom, L.; Schleyer, P. v. R.; Pople, J. A. *Ab Initio Molecular Quantum Theory*; Wiley: New York, 1986.
(58) Frisch, M. J.; Trucks, G. W.; Schlegel, H. B.; Scuseria, G. E.; Robb, M. A.; Cheeseman, J. R.; Scalmani, G.; Barone, V.; Mennucci, B.; Petersson, G. A.; Nakatsuji, H.; Caricato, M.; Li, X.; Hratchian, H. P.; Izmaylov, A. F.; Bloino, J.; Zheng, G.; Sonnenberg, J. L.; Hada, M.; Ehara, M.; Toyota, K.; Fukuda, R.; Hasegawa, J.; Ishida, M.; Nakajima, T.; Honda, Y.; Kitao, O.; Nakai, H.; Vreven, T.; Montgomery, J. A., Jr.; Peralta, J. E.; Ogliaro, F.; Bearpark, M.; Heyd, J. J.; Brothers, E.; Kudin, K. N.; Staroverov, V. N.; Kobayashi, R.; Normand, J.; Raghavachari, K.; Rendell, A.; Burant, J. C.; Iyengar, S. S.; Tomasi, J.; Cossi, M.; Rega, N.; Millam, J. M.; Klene, M.; Knox, J. E.; Cross, J. B.; Bakken, V.; Adamo, C.; Jaramillo, J.; Gomperts, R.; Stratmann, R. E.; Yazyev, O.; Austin, A. J.; Cammi, R.; Pomelli, C.; Ochterski, J. W.; Martin, R. L.; Morokuma, K.; Zakrzewski, V. G.; Voth, G. A.; Salvador, P.; Dannenberg, J. J.; Dapprich, S.; Daniels, A. D.; Farkas, O.; Foresman, J. B.; Ortiz, J. V.; Cioslowski, J.; Fox, D. J. *Gaussian 09*; Gaussian, Inc.: Wallingford, CT, 2009.
(59) Gil, A.; Branchadell, V.; Bertran, J.; Oliva, A. *J. Phys. Chem. B* **2009**, *113*, 4907−4914.
(60) Acosta-Silva, C.; Branchadell, V.; Bertran, J.; Oliva, A. *J. Phys. Chem. B* **2010**, *114*, 10217−10227.
(61) Olson, W. K.; Bansal, M.; Burley, S. K.; Dickerson, R. E.; Gerstein, M.; Harvey, S. C.; Heinemann, U.; Lu, X.-J.; Neidle, S.; Shakked, Z.; Sklenar, H.; Suzuki, M.; Tung, C.-S.; Westhof, E.; Wolberger, C.; Berman, H. M. *J. Mol. Biol.* **2001**, *313*, 229−237.
(62) Boys, S. F.; Bernardi, F. *Mol. Phys.* **1970**, *19*, 553−566.
(63) Simon, S.; Duran, M.; Dannenberg, J. J. *J. Chem. Phys.* **1996**, *105*, 11024−31.
(64) Šponer, J.; Leszczynski, J.; Hobza, P. *Biopolymers* **2002**, *61*, 3−31.
(65) Reed, A. E.; Weistock, R. B.; Weinhold, F. *J. Chem. Phys.* **1985**, *73*, 735−746.
(66) Reed, A. E.; Curtiss, L. A.; Weinhold, F. *Chem. Rev.* **1988**, *88*, 899−926.
(67) Glendening, E. D.; Badenhoop, J. K.; Reed, A. E.; Carpenter, J. E.; Bohmann, J. A.; Morales, C. M.; Weinhold, F. *NBO 5.0*; Theoretical Chemistry Institute, University of Winsconsin: Madison, WI, 2001.
(68) Bader, R. F. W. *Atoms in Molecules: A Quantum Theory*; Clarendon: Oxford, UK, 1990.
(69) Friedrich Biegler-König, J. S. *J. Comput. Chem.* **2002**, *23*, 1489−1494.
(70) te Velde, G.; Bickelhaupt, F. M.; van Gisbergen, S. J. A.; Fonseca Guerra, C.; Baerends, E. J.; Snijders, J. G.; Ziegler, T. *J. Comput. Chem.* **2001**, *22*, 931−967.
(71) Fonseca Guerra, C.; Snijders, J. G.; te Velde, G.; Baerends, E. *J. Theor. Chem. Acc.* **1998**, *99*, 391−403.
(72) *ADF2013*; SCM, Theoretical Chemistry; Amsterdam, The Netherlands. http://www.scm.com.
(73) Kitaura, K.; Morokuma, K. *Int. J. Quantum Chem.* **1975**, *10*, 325−340.
(74) von Hopffgarten, M.; Frenking, G. *Wiley Interdiscip. Rev.: Comput. Mol. Sci.* **2012**, *2*, 43−63.
(75) Zaho, Y.; Truhlar, D. G. *J. Chem. Phys.* **2006**, *125*, 194101.
(76) Becke, A. D. *J. Chem. Phys.* **1993**, *98*, 5648−5652.
(77) Miehlich, B.; Savin, A.; Stoll, H.; Preuss, H. *Chem. Phys. Lett.* **1989**, *157*, 200−206.
(78) Lee, C.; Yang, W.; Parr, G. *Phys. Rev. B: Condens. Matter* **1988**, *37*, 785−789.
(79) Grimme, S.; Antony, J.; Ehrlich, S.; Krieg, H. *J. Chem. Phys.* **2010**, *132*, 154104.
(80) Hobza, P.; Šponer, J.; Leszczynski, J. *J. Phys. Chem. B* **1997**, *101*, 8038−8039.

DOI: 10.1021/ct5006104
J. Chem. Theory Comput. 2015, 11, 2714−2728

(81) Lin, I.-C.; von Lilienfeld, O. A.; Coutinho-Neto, M. D.; Tavernelli, I.; Rothlisberger, U. *J. Phys. Chem. B* **2007**, *111*, 14346−14354.
(82) Korth, M.; Pitoňák, M.; Řezáč, J.; Hobza, P. *J. Chem. Theory Comput* **2010**, *6*, 344−352.
(83) Stewart, J. J. P. *MOPAC2012*, version 14.083L; Stewart Computational Chemistry: Colorado Springs, CO. http://openmopac.net.
(84) Maia, J. D. C.; Carvalho, G. A. U.; Mangueira, C. P., Jr.; Santana, S. R.; Cabral, L. A. F.; Rocha, G. B. *J. Chem. Theory Comput.* **2012**, *8*, 3072−3081.
(85) Strutyński, K.; Gomes, J. A. N. F.; Melle-Franco, M. *J. Phys. Chem. A* **2014**, *118*, 9561−9567.
(86) Gil, A.; Melle-Franco, M.; Branchadell, V.; Calhorda, M. J. To be submitted for publication.
(87) Ganem, B.; Li, Y.-T.; Henion, J. D. *Tetrahedron Lett.* **1993**, *34*, 1445−1448.
(88) Rueda, M.; Kalko, S. G.; Luque, F. J.; Orozco, M. *J. Am. Chem. Soc.* **2003**, *125*, 8007−8014.
(89) Robertazzi, A.; Platts, J. A. *J. Phys. Chem. A* **2006**, *110*, 3992−4000.
(90) Hill, G.; Forde, G.; Hill, N.; Lester, W. A.; Sokalski, A. W.; Leszczynski, J. *Chem. Phys. Lett.* **2003**, *381*, 729−732.
(91) Pierre, V. C.; Kaiser, J. T.; Barton, J. K. *Proc. Natl. Adad. Sci. U.S.A.* **2007**, *104*, 429−434.
(92) Wei, D. G.; Wilson, W. D.; Neidle, S. *J. Am. Chem. Soc.* **2013**, *135*, 1369−1377.
(93) Hall, J. P.; Cook, D.; Ruiz Morte, S.; McIntyre, P.; Buchner, K.; Beer, H.; Cardin, D. J.; Brazier, J. A.; Winter, G.; Kelly, J. M.; Cardin, C. J. *J. Am. Chem. Soc.* **2013**, *135*, 12652−12659.
(94) Slifkin, M. A. *Charge-Transfer Interactions of Biomolecules*; Academic Press: New York, 1971.
(95) Coates, C. G.; Callaghan, P.; McGarvey, J. J.; Kelly, J. M.; Jacquet, L.; Kirsch-De Mesmaeker, A. *J. Mol. Struct.* **2001**, *598*, 15−25.
(96) Ortmans, I.; Elias, B.; Kelly, J. M.; Moucheron, C.; Kirsch-DeMesmaeker, A. *Dalton Trans.* **2004**, 668−676.
(97) Elias, B.; Creely, C.; Doorley, G. W.; Feeney, M. M.; Moucheron, C.; Kirsch-DeMesmaeker, A.; Dyer, J.; Grills, D. C.; George, M. W.; Matousek, P.; Parker, A. W.; Towrie, M.; Kelly, J. M. *Chem.—Eur. J.* **2008**, *14*, 369−375.
(98) Very, T.; Despax, S.; Hébraud, P.; Monari, A.; Assfeld, X. *Phys. Chem. Chem. Phys.* **2012**, *14*, 12496−12504.
(99) Chantzis, A.; Very, T.; Daniel, C.; Monari, A.; Assfeld, X. *Chem. Phys. Lett.* **2013**, *578*, 133−137.
(100) Chantzis, A.; Very, T.; Dexpax, S.; Issenhuth, J.-T.; Boeglin, A.; Hébraud, P.; Pfeffer, M.; Monari, A.; Assfeld, X. *J. Mol. Model.* **2014**, *20*, 2082.
(101) Véry, T.; Ambrosek, D.; Otsuka, M.; Gourlaouen, C.; Assfeld, X.; Monari, A.; Daniel, C. *Chem.—Eur. J.* **2014**, *20*, 12901−12909.
(102) Dewar, M. J. S.; Lepley, A. R. *J. Am. Chem. Soc.* **1961**, *83*, 4560−4563.
(103) Mulliken, R. S.; Person, W. B. *Molecular Complexes*; Wiley-Interscience: New York, 1969.
(104) Bader, R. F. W. *Chem. Rev.* **1991**, *91*, 893−928.
(105) Bader, R. F. W.; Essen, H. *J. Chem. Phys.* **1984**, *80*, 1943−1960.
(106) Estévez, L.; Otero, N.; Mosquera, R. *J. Phys. Chem. A* **2009**, *113*, 11051−11058.
(107) Zhikol, O.; Shishkin, O.; Lyssenko, K.; Leszczynski, J. *J. Chem. Phys.* **2005**, *122*, 144104.
(108) Gil, A.; Branchadell, V.; Bertran, J.; Oliva, A. *J. Phys. Chem. B* **2007**, *111*, 9372−9379.
(109) Snyder, R. D. *Mutat. Res., Fundam. Mol. Mech. Mutagen.* **2007**, *623*, 72−82.
(110) Riahi, S.; Eynollahi, S.; Ganjali, M. R. *Chem. Biol. Drug. Des.* **2010**, *76*, 425−432.

DOI: 10.1021/ct5006104
J. Chem. Theory Comput. 2015, 11, 2714−2728